

# A Process to Produce Battery Grade Silicon from Natural Halloysite Clay

Nathan Clarke<sup>1</sup>, Wenquan Lu<sup>3</sup>, Senpei Zhang<sup>3</sup>, Brian Mazzeo<sup>2</sup>, Rickey Taylor<sup>2</sup>, and Dean Wheeler<sup>1</sup>

<sup>1</sup> Chemical Engineering Department Brigham Young University

<sup>2</sup> Electrical Engineering Department Brigham Young University

<sup>3</sup> Argonne National Lab

## Abstract

*We demonstrate the production of silicon from a clay mineral, halloysite, as a low-cost silicon source for high-energy anodes in aviation batteries. The halloysite-derived silicon demonstrated 1800 mAh/g capacity after formation cycles, comparable to other developing silicon materials.*

## Introduction

Silicon has 10 times the theoretical capacity of graphite, which is often used as the active material in Li-ion battery anodes. Materials with higher capacity are needed to enable electrified flight. Various methods have been developed to produce electrochemically active silicon for anode use, however, the processes tend to be expensive [1, 2]. We demonstrate the use of halloysite, a clay mineral, as a source for low-cost nano-structured silicon.

The use of halloysite to produce silicon utilizes the unique structure the mineral already possesses, as shown in Figure 1. Our experiments were designed to preserve that structure, which also provides the potential for lower-cost production.

Deriving silicon from halloysite with the desired structure required the development of a reactor system with tailored safety features. The design also has the ability to decrease cost by recycling materials that do not participate in the reaction.

## Background

For many years, the potential benefit of using silicon as the active material in anodes has been recognized. The challenge lies in that silicon experiences massive changes in volume during cycling, on the order of 300%. Such expansion and contraction produce structural deformation that leads to capacity fade [3, 4].

The unique morphology of halloysite may provide stability during cycling. The mineral forms a tubular/cylindrical shape, with a chemical formula of  $\text{Al}_2\text{Si}_2\text{O}_5(\text{OH})_4 \cdot n(\text{H}_2\text{O})$ , a polymorph of kaolinite. We are using halloysite that was mined locally near Eureka, Utah as our silicon source.

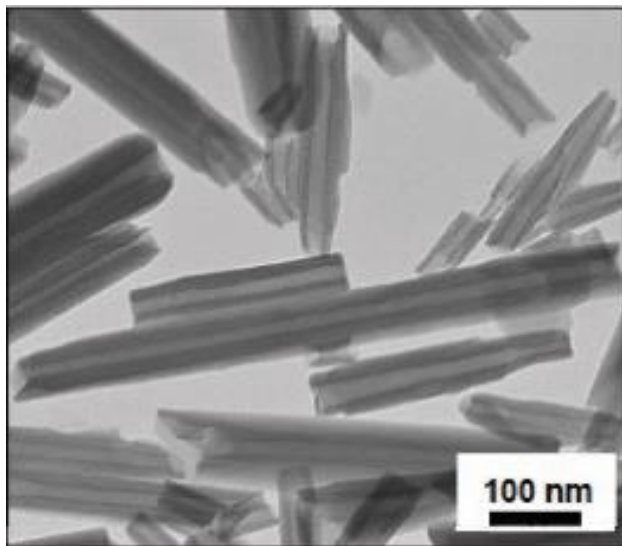


**Figure 1**  
TEM image of halloysite. The tubular nature of the material is clear with an inner diameter on the order of 20-30nm the outer diameter between 50-100nm.

Often silicon is produced through the reduction of silica ( $\text{SiO}_2$ ). In this instance, halloysite will first be etched to remove everything but the silica in preparation for reduction. The reduction process can be carried out by placing silica in the presence of a metal that has a lower redox potential than silicon such as aluminum (Al) and magnesium (Mg). Magnesium is used here because it has a lower redox potential than aluminum, though aluminum has been used by other researchers [5, 6]. The process is very exothermic, though a large energy barrier prevents the initiation of the reaction at room temperature [5]. This magnesiothermic (or aluminothermic) reduction is not new, though we show some

improvements to the process in both safety and higher yield.

Because the reduction reaction is exothermic a salt is needed to prevent thermal runaway. The salt dilutes the reactants and provides thermal mass to absorb and conduct the heat that is produced in the exothermic reaction [7]. The salt needs to be molten to provide the needed heat transfer and diffusion of reactants. Various salts have been used in the past. We will use aluminum chloride ( $\text{AlCl}_3$ ) because of its low melting point,  $192^\circ\text{C}$ , and it can be reclaimed at the end of the reaction. Aluminum chloride has a relatively high vapor pressure, compared to other salts, which can allow for sublimation of the salt in order to remove it from the reaction products. The vapor can be collected, allowing the salt to be recycled.

The lower melting point of aluminum chloride allows the reaction to take place at lower temperatures, providing potential structural benefits. The lower temperatures leads to less crystallinity in the final silicon product [6]. Amorphous silicon may provide ions an increased ability to diffuse in and out of the particles during cycling.

## Reactor Design and Safety

We designed a new reactor for safer processing. The safety concerns include runaway reaction, volume expansion of the salt due to melting, and inert containment in the case of either of the previous issues occurring. Previous publications mention the use of a hydrothermal autoclave reactor [5, 7, 8]. Autoclave reactors provide the ability to carry out experiments in a controlled atmosphere with temperatures up to  $250^\circ\text{C}$  and have an inert liner. The reactors are able to release gasses if pressure exceeds design. However, the reactors use conventional

pressure relief which cannot safely release a solid or viscous liquid if the pressure exceeds design.

The molten salt with the material dissolved or suspended within it is very viscous and would not be able to be released in case of an accident. The salt also is unique in the volume change experienced during melting. According to the DIPPR database the liquid salt may have a volume as much as double the solid volume [9]. This could pose a serious safety hazard if the reactor is loaded more than half full due to hydrostatic pressure exceeding limits of the vessel.

We modified the reactor to still use components from the hydrothermal

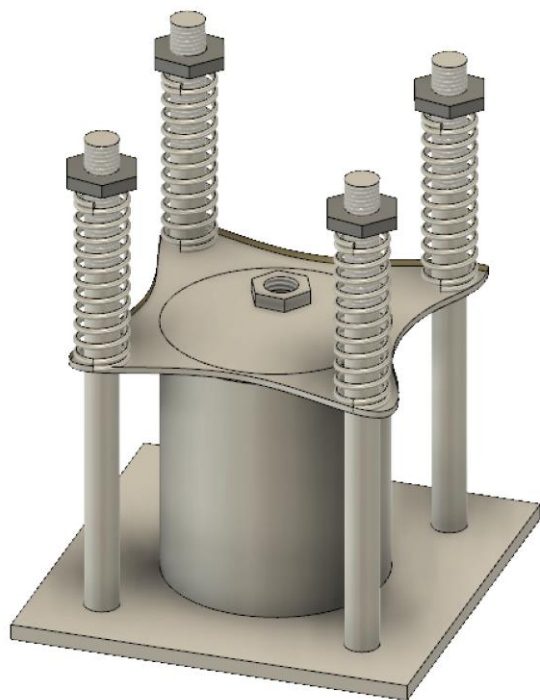


**Figure 2**

This CAD concept of the reactor shows the key components. The springs push against a steel plate that transfers the force of the springs onto the lid of the vessel that holds the reactants. This feature is the key safety mechanism that prevents excess pressure build up. The hole in the top of the reactor is a thermowell that will allow for temperature measurements within the vessel. The vessel is contained in a steel shell that provides structural stability while hot and under pressure.

autoclave reactor, though the threaded lid is not used. Instead, we made a containment system that uses high temperature springs to provide the pressure needed to hold the reactor closed, as shown in Figure 2. These springs are compressed to a given force, ensuring that the reactor opens at a given pressure. The system was tested with water at multiple temperatures to ensure the reactor would open at a desired pressure.

In the unfortunate event of material leaving the reactor vessel, hot magnesium could be exposed to oxygen in the air. The use of a lower temperature process decreases the chance of ignition, though out of an abundance of caution the oven that is heating the vessel is also purged with nitrogen gas.

## Methods

### *Acid Etching of Halloysite*

The first step in the process is to remove all the aluminum with their respective oxygens (alumina) as well as the hydroxides. To do so, 35 g of halloysite is placed in 350 ml of 4 molar HCl and slowly heated to 110°C while being stirred. The contents are stirred at temperature for a minimum of 5 h.

The product is washed with deionized water by allowing the solid to settle and decanting the liquid until a pH >5 is reached. The powder is then filtered and washed again to ensure all dissolved material is removed. The powder is dried in an oven at 90°C for 10 h.

### *Silica Powder Pellet Prep*

Dried silica powder is brought into a glovebox to be mixed with magnesium and aluminum chloride. The need for an inert

atmosphere comes from both magnesium and aluminum chloride. The surface of magnesium oxidizes rapidly when exposed to oxygen, decreasing the effectiveness of magnesium as a reducing agent. Aluminum chloride is sensitive to water, reacting to form HCl vapor, as shown below:

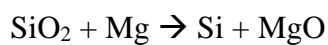


The three powders are mixed through stirring as well as mortar and pestle. Aluminum chloride, silica, and magnesium are mixed in a mass ratio of 45:5:4, respectively. Other researchers have published a ratio of 40 for aluminum chloride [10], however, this ratio is very close to the line where a runaway reaction can happen. We have chosen to increase the relative amount of the salt and will show that there is not detrimental impact to the overall yield.

A pellet is produced by compressing the mixed powder in a 20-ton press. The powder is left under full pressure for 30 minutes before being removed. The pellets are loaded into the reactor vessel and closed in the glovebox, to keep an inert atmosphere throughout the reaction. The importance of making a pellet will be discussed below.

### Reduction

The reactor vessel is setup in the reactor previously described. The springs are compressed to open at 8 atm, the vapor pressure within the vessel should reach 6.5 atm. The oven is then closed and purged with argon. The oven is slowly ( $2.5^\circ\text{C}/\text{min}$ ) taken to  $250^\circ\text{C}$  and held there for 12 h. The reduction reaction is:



### Separation

After the reduction step is complete the contents of the vessel have solidified, DI water is used to dissolve out the aluminum chloride allowing the other contents to be dispersed in water. The contents are then washed with 4 molar HCl to dissolve the magnesium oxide. The material is further washed with DI water, separated via centrifuging, until  $\text{pH} > 6$  is achieved. The resultant powder is dried at  $150^\circ\text{C}$  for 5 h. The resultant powders are shown in Figure 3.

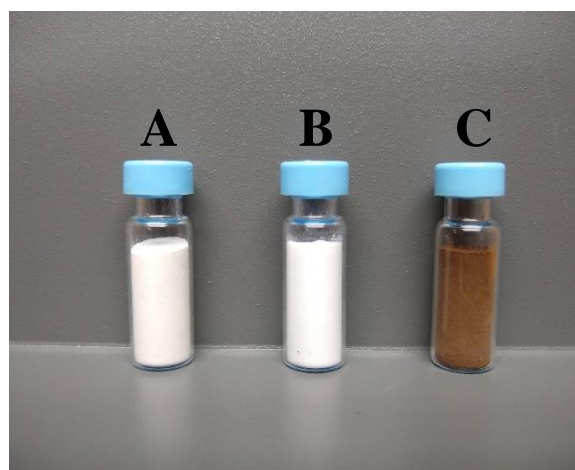


**Figure 3**  
The three stages the powder exists in. A) is pure halloysite from Dragon Mine. B) is silica produced from halloysite. C) is the final silicon powder.

### SEM

A scanning electron microscope (SEM) was used to understand the morphological changes that took place through the process.

### XRD Spectra

X-ray Diffraction (XRD) is used to determine the purity and relative crystallinity of the silicon produced. Other processes use HF acid to dissolve residual silica. To decrease cost and lower any risk associated with production we do not use



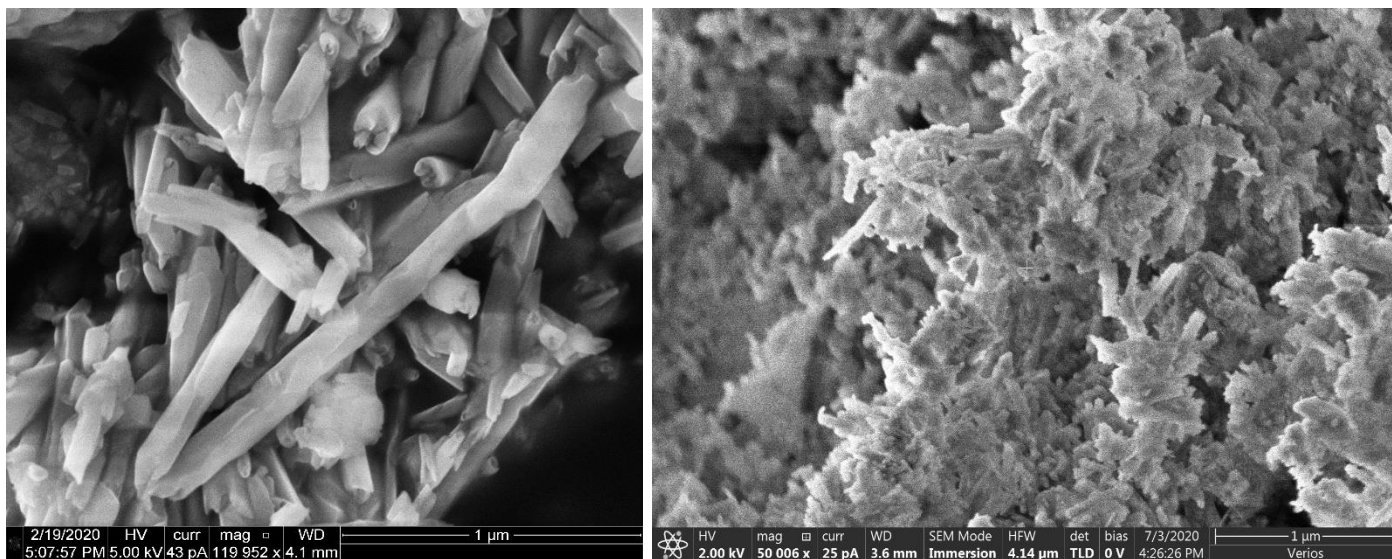


**Figure 4**

The above images are SEM photomicrographs of pure halloysite on the left and our silicon derived from halloysite on the right. The cylindrical nature of the mineral is preserved throughout processing, though the hollow nature seems to have been lost.

HF acid. Without the treatment there will be some residual silica remaining. The diffraction pattern given by silica and silicon are notably different and can easily be differentiated and quantified. Crystallinity can be qualitatively determined, though without a standard to measure against the quantitative analysis is not preformed.

#### *Battery Performance*

Halloysite-derived silicon was tested at Argonne National Lab (ANL). Pouch cells were made with a cathode active material of NMC (lithium nickel manganese cobalt oxide). Silicon was mixed with carbon additive and binder to make a conventional 70 wt% Si anode.

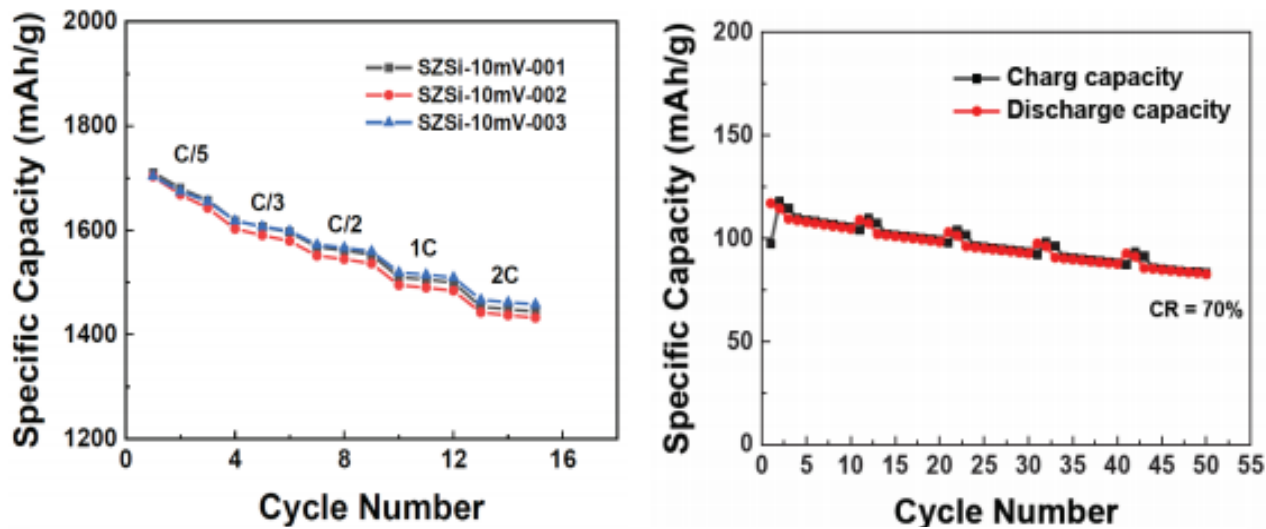


**Figure 5**

The above shows cycling data for halloysite-derived silicon. On the left a graph showing the performance of the material at different rates. On the right is a graph demonstrating that the capacity retention is around 70% at 50 cycles.

## Results

The process produces a dark brown powder in the end. This is a clear distinction from the white silica and tan halloysite, as shown in Figure 3. The powders are all very hydrophilic, which required much longer drying times than initially thought. Even pure halloysite contains 4.1% by mass water.

## SEM

Following the procedures previously discussed silicon was produced from halloysite, as shown in Figure 4. The tubular morphology was lost, though the cylindrical nature of the particles was maintained. The particles are approximately 1  $\mu\text{m}$  in length and 50-100 nm diameter.

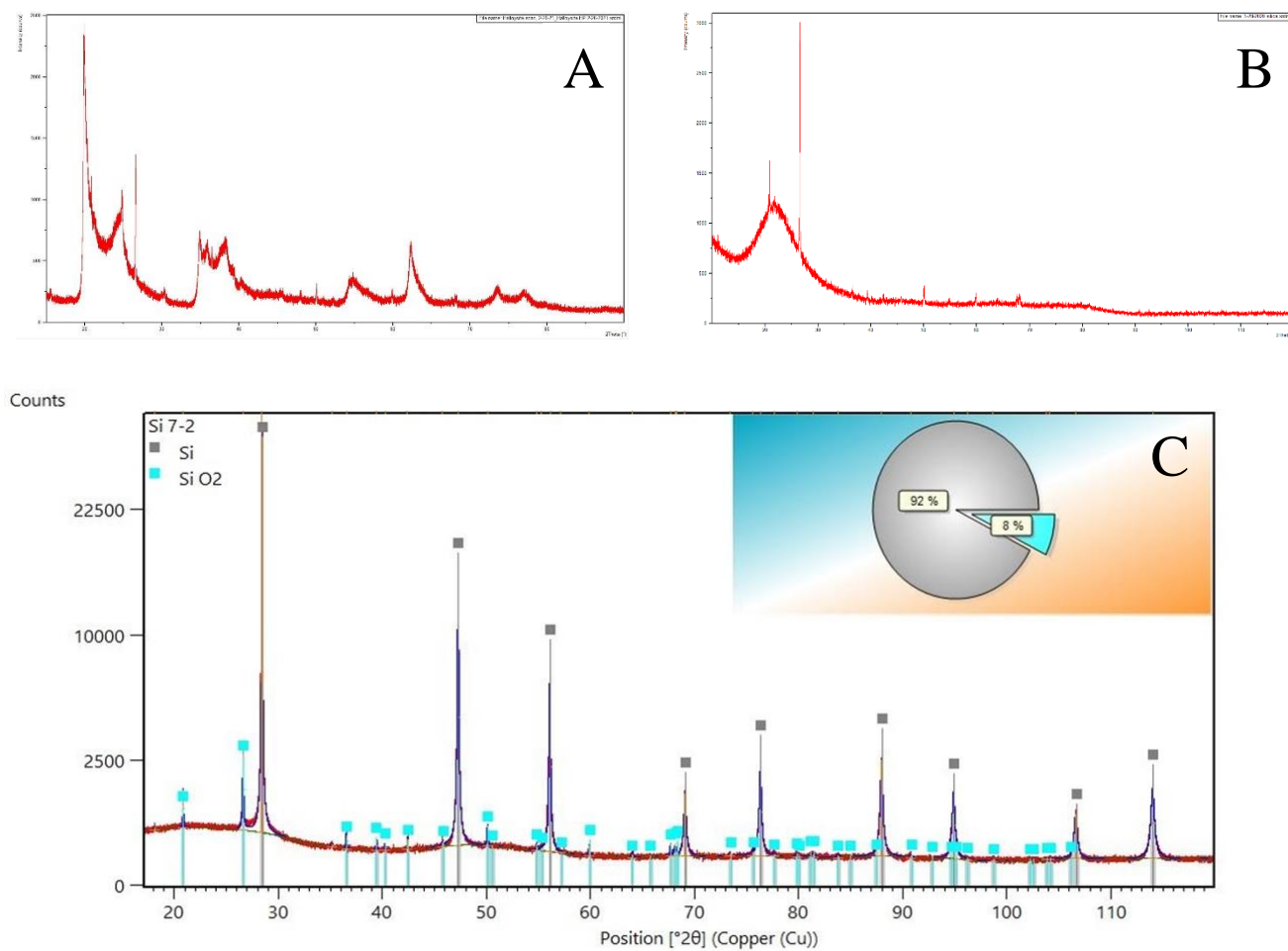


**Figure 6**

XRD spectra of the three different powders. All three spectra display the square of the counts, which can help emphasize peak morphology. A) is the spectra of pure halloysite. B) is the spectra of halloysite-derived silica. Of note is the large lump of the lower angles, this is indicative of the amorphous nature of the silica produced from halloysite. C) is the spectra of the halloysite-derived silicon. The graph in the upper right shows the composition of the final product as being 92% silicon and 8% silica, the respective peaks are indicated by the legend on the upper left.

### *Cycling Performance*

The full cells were cycled 50 times as well as tested at different rates of charge/discharge. Figure 5 shows the results of those experiments. These results are on par with other silicon materials tested by ANL, showing that the material is electrochemically active and has potential for future optimization as an anode material.

### *XRD*

When the XRD spectra data were analyzed to determine what percent of silica remained. Before mortar and pestle was used and the powder pressed into a pellet, the residual silica was as high as 25%. Once improvements were made to mixing and the creation of a pellet the residual silica was lowered to as low as 8%, see figure 5. This is higher than other published yields, which were only able to achieve 25% residual silica.

A lack of crystallinity is thought to provide more pathways for lithium ions to diffuse through a solid particle, which happens during cycling. We are unfortunately unable to qualitatively measure the amount of crystalline vs amorphous materials at this point. However, we can see qualitative indicators in the spectra. Figure 6B shows a wide peak at the lower angles or the silica spectrum, indicative of amorphous material [11]. In the final silicon the wide peak is much smaller, indicating an increase in crystallinity. The wide peak at the lower angles may just be due to the residual silica. There is also a slight peak between 45-60  $2\theta$  that could indicate a new source of amorphous material. There are potential ways of quantifying the amount of crystallinity using NMR (nuclear magnetic resonance) [12], though we do not present that here.

### **Conclusion**

Halloysite-derived silicon shows promise as a low-cost anode material for use in Li-ion batteries. The process and reactor we have developed provide a safe way to produce electrochemically active silicon. With a capacity of 1800 mAh/g the material may be able to provide the needed capacity for electric flight. The process needs to be optimized, there may be changes that could lower the cost of production or enhance the structural stability of the material. The material also needs to be tested for more than just 50 cycles to determine how stable the material is.

### **Acknowledgments**

We are gratefully for and acknowledge the Utah NASA Space Grant Consortium for funding this work.

W. L. from Argonne National Laboratory (ANL) gratefully acknowledges the support from the U.S. Department of Energy's (DOE) office of Energy Efficiency & Renewable Energy (EERE) Vehicle Technologies Office. ANL is a U.S. Department of Energy Office of Science Laboratory operated under Contract No. DE-AC02-06CH11357.

### **References**

1. Hieu, N.S., J.C. Lim, and J.K. Lee, *Free-standing silicon nanorods on copper foil as anode for lithium-ion batteries*. *Microelectronic Engineering*, 2012. **89**: p. 138-140.
2. Youn, D.-Y., et al., *Stable and High-Capacity Si Electrodes with Free-Standing Architecture for Lithium-*

- Ion Batteries*. ACS Applied Energy Materials, 2020. **3**(1): p. 208-217.
3. Canham, L., *Porous Silicon Formation by Porous Silica Reduction*, in *Handbook of Porous Silicon*, L. Canham, Editor. 2014, Springer International Publishing: Cham. p. 85-92.
  4. Beattie, S.D., et al., *Understanding capacity fade in silicon based electrodes for lithium-ion batteries using three electrode cells and upper cut-off voltage studies*. Journal of Power Sources, 2016. **302**: p. 426-430.
  5. Lin, N., et al., *A low temperature molten salt process for aluminothermic reduction of silicon oxides to crystalline Si for Li-ion batteries*. Energy & Environmental Science, 2015. **8**(11): p. 3187-3191.
  6. Lai, Y., J.R. Thompson, and M. Dasog, *Metallothermic Reduction of Silica Nanoparticles to Porous Silicon for Drug Delivery Using New and Existing Reductants*. Chemistry – A European Journal, 2018. **24**(31): p. 7913-7920.
  7. Zhou, X., et al., *Synthesis of nano-sized silicon from natural halloysite clay and its high performance as anode for lithium-ion batteries*. Journal of Power Sources, 2016. **324**: p. 33-40.
  8. Du, Y., et al., *Si/graphene composite prepared by magnesium thermal reduction of SiO<sub>2</sub> as anode material for lithium-ion batteries*. Electrochemistry Communications, 2013. **36**: p. 107-110.
  9. <https://dippr.aiche.org/FullDb>.
  10. Wan, H., et al., *Three-dimensionally interconnected Si frameworks derived from natural halloysite clay: a high-capacity anode material for lithium-ion batteries*. Dalton Transactions, 2018. **47**(22): p. 7522-7527.
  11. Ohlberg, S.M. and D.W. Strickler, *Determination of Percent Crystallinity of Partly Devitrified Glass by X-Ray Diffraction*. Journal of the American Ceramic Society, 1962. **45**(4): p. 170-171.
  12. Radhakrishnan, S., et al., *Trace Level Detection and Quantification of Crystalline Silica in an Amorphous Silica Matrix with Natural Abundance <sup>29</sup>Si NMR*. Analytical Chemistry, 2020. **92**(19): p. 13004-13009.